© 2014,
Scienceline Publication
www.science-line.com

ISSN: 2322-5114
Journal of World's Electrical Engineering and Technology
J. World. Elect. Eng. Tech. 3(1): 37-46, 2014

JWEET

Voltage Sag Evaluation during Induction Motors Starting Using Artificial Neural Network

Alireza Sadoughi[1] and Iman Sadeghkhani[2]*

[1]Department of Electrical Engineering, Malek-Ashtar University of Technology, Shahinshahr 115/83145, Iran
[2]Department of Electrical Engineering, Najafabad Branch, Islamic Azad University, Najafabad 85141-43131, Iran

*Corresponding author's Email: i.sadeghkhani@ec.iut.ac.ir

Abstract *– One of the most important concerns in electrical systems is to deliver energy to the consumers with high power quality (PQ). Because of great importance of voltage sag among all PQ events, this paper presents evaluation of voltage sags caused by induction motors (IMs) starting. Malfunctioning or failure of sensitive loads is main effect of this phenomenon. Both depth and duration of voltage sag are evaluated in this work using artificial neural network (ANN). Both multilayer perceptron (MLP) and radial basis function (RBF) structures have been analyzed. Six learning algorithms, backpropagation (BP), delta-bar-delta (DBD), extended delta-bar-delta (EDBD), directed random search (DRS), quick propagation (QP), and levenberg marquardt (LM) were used to train the MLP. The simulation results show that proposed technique can estimate the voltage sag characteristics with good accuracy. Also, it is shown that the LM and EDBD algorithms present better performance for evaluating of voltage sag magnitude and duration.*

Keywords*: Induction Motors, Multilayer Perceptron, Motor Cable, Radial Basis Function, Voltage Sag*.

ORIGINAL ARTICLE
Received 14 Jan. 2014
Accepted 05 Mar. 2014

INTRODUCTION

The study of power quality (PQ) disturbances continues to receive remarkable attention because of additive utilization of voltage sensitive equipment and power electronic devices. In other words, due to incremental sensitivity of customer equipment and their awareness about effect of small variation in the quality of electrical supply, quality of electricity service must be as high as possible. The main power quality disturbances are harmonics, inter-harmonics, voltage sag/swell, voltage flicker, frequency fluctuations, noise, notch, transient overvoltages, voltage interruption, and voltage unbalance. Among all of them, voltage sag is one of the most frequent causes of equipment malfunctions and costly disruptions of industrial processes [1-7].

According to the IEC 61000-4-30 standard, voltage sag (dip) is defined as "a temporary reduction of the voltage at a point of the electrical system below a threshold" [8]. This threshold is determined by the IEEE 1159-1995 standard as 90% of the nominal voltage [9]. The latter standard defines voltage sag as reduction in root mean square (RMS) voltage between 0.1-0.9 p.u. for a time greater than 0.5 cycles to one minute at power frequency. The main causes of voltage sags are faults and inrush currents due to motor starting/transformer energization. In this paper, voltage sags caused by induction motors (IMs) starting is investigated because these motors are widely used in the various sections of the world including industrial, domestic, educational sections, etc. [10-11].

One of the steps for improving power quality is measurement of PQ disturbances. For this purpose, this paper proposes an intelligent approach to estimate voltage sag during IMs starting. In this paper power system blockset (PSB), a MATLAB/Simulink-based simulation tool, is used for calculation of voltage sag [12]. In order to study various conditions of starting an IM, many possible system configurations must be considered which needs many time-domain simulations resulting in a large amount of simulation time. This paper presents a real-time estimator for voltage sags. The artificial neural network (ANN) is used as intelligent tool for this purpose. A tool such as proposed in this paper that can give the voltage sag characteristics will be helpful to the manufactures and operators during design and operation stages. The ANN is trained with the most commons structures and algorithms. In the proposed estimator, we have considered the most important aspects which influence the voltage sag such as supply voltage, cable resistance and reactance, stator/rotor resistance and reactance, load torque and total inertia. This information will help the companies and operators to design and handle IMs and sensitive loads safely with voltage sags appearing safe within the limits. Results of the studies

To cite this paper: Sadoughi A. and Sadeghkhani I. 2014. Voltage Sag Evaluation during Induction Motors Starting Using Artificial Neural Network. *J World Elec. Eng. Tech.*, 3 (1): 37-46.
Journal homepages: http://www.jweet.science-line.com/

show that developed ANNs can estimate voltage sags caused by induction motors starting with good accuracy.

STUDY SYSTEM MODELLING

A. Induction Machine

The electrical section of induction machine is represented by a fourth-order state-space model and the mechanical section by a second-order system [13]. All electrical variables and parameters are referred to the stator. All stator and rotor quantities are in the arbitrary two-axis reference frame (d-q frame).

B. Connecting Cable

Usually cables are modeled using series resistance and inductance and parallel capacitance in the distributed form or in the PI form [14]. Since cable length between IM and its supply is short (in comparison with high-voltage transmission cables) and therefore value of parallel capacitor is low, effect of this capacitance on the voltage sag is small; therefore this capacitance can be neglected in this evaluation. Simulation results, shown in Fig. 1, also verify that this capacitance has negligible effect on the voltage sag depth and duration. This capacitor has significant effect in the transient studies of induction machines [15]. Therefore, connecting cable is modeled by a series equivalent resistance and reactance.

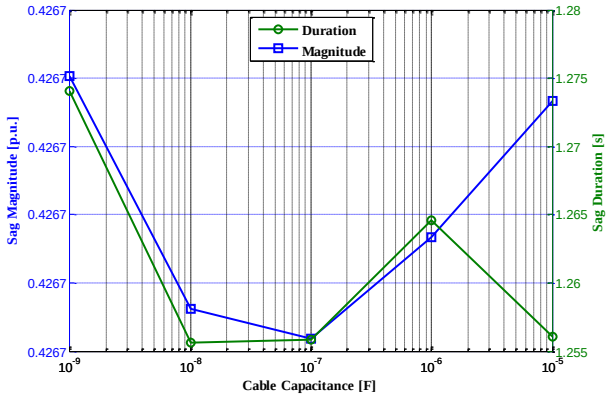

Fig. 1 - Voltage sag magnitude and duration as cable capacitance. All other parameters are fixed.

VOLTAGE SAG CHARACTERISTICS

Voltage sag caused by IMs starting current is one of the main causes of sensitive equipment dropout [3]. Thus, this phenomenon should be evaluated accurately. As mentioned above, RMS voltage reduction by 10%-90% of rated voltage with duration from half a cycle to 1 min is called voltage sag. Based on this definition, a voltage sag has two main characteristics: magnitude (depth) and duration. A typical voltage sag characteristics is shown in Fig. 2. The magnitude of voltage sag can determine in a number of ways. The most common approach to obtain the sag magnitude is to use RMS voltage, which is adopted in this paper. If the magnitude of the voltage drops below 10% of the nominal voltage, the disturbance is classified as an interruption [1]. In the other hand, the duration of a voltage sag is the amount of time during which the voltage magnitude is below threshold which is typically chosen as 90% of the nominal voltage magnitude.

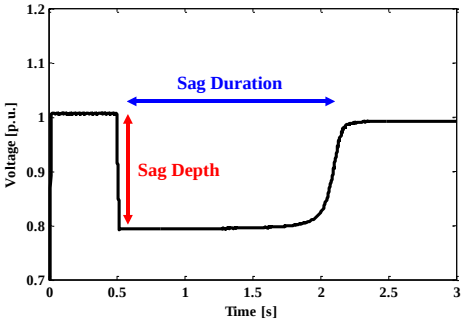

Fig. 2 - A typical voltage sag characteristics.

The sample system considered for explanation of the proposed methodology consists a large induction motor which produces notable starting current. Thus, voltage sag phenomenon is more obvious. This system is shown in Fig. 3. For this purpose, induction motor KHV355-2 from VALIADIS company was considered [16]. It is a 2 poles, 200 kW (270 hp), 3300 V induction motor which is in the medium-voltage category. Parameters of this motor were calculated using no-load test, locked-rotor test, and DC test [17]. This motor is fully simulated in the MATLAB software [12]. Fig. 4 shows voltage sags at bus 2 caused by IM starting for all three phases. This disturbance can affect operation of sensitive loads connected to bus 2 (for example industrial loads).

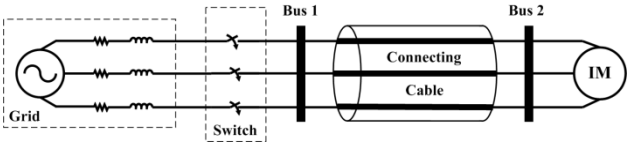

Fig. 3 - Sample system for the voltage sag study.

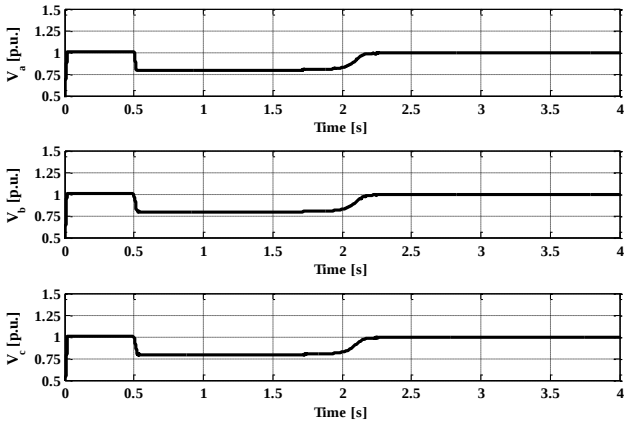

Fig. 4 - Three-phase voltage at bus 2. IM starts at t= 0.5 s.

In practical system a number of factors affect the voltage sag. In this paper following parameters were considered:

- Supply voltage (V)
- Equivalent resistance of the connecting cable (R_c)
- Equivalent reactance of the connecting cable (X_c)
- Stator resistance (R_s)
- Stator reactance (X_{ls})
- Referred rotor resistance (R'_r)
- Referred rotor reactance (X'_{lr})
- Load torque (T_L)
- Total rotor and load inertia (J)

In this section, effect of each parameter on the voltage sag characteristics is presented. First, Fig. 5 shows the effect of supply voltage on the voltage sag. In this work, adopted voltage sag is the worst case of sag among all three phases. Effect of cable resistance variation on the voltage sag depth and duration is shown in Fig. 6. As shown in this figure, cable reactance more affects sag depth and doesn't has major effect on the sag duration. In addition, Fig. 7 shows the effect of cable reactance on the voltage sag. Unlike cable resistance, this parameter affects both depth and duration significantly. Effect of stator resistance and reactance on the voltage sag is shown in Figs. 8 and 9, respectively. As shown in these figures, stator resistance only affects sag duration significantly, while stator reactance affects both depth and duration of voltage sag. Also, Figs. 10 and 11 show the effect of referred rotor resistance and reactance on the voltage sag characteristics, respectively. Effect of rotor parameters on the voltage sag is similar to effect of stator parameters. Load torque also affects the voltage sag as shown in Fig. 12. Moreover, effect of total rotor and load inertia on the voltage sag characteristics is shown in Fig. 13. As shown in Figs 12 and 13, the higher the load torque and total inertia, the more the voltage sag duration.

There are other parameters which not considered here for evaluation of voltage sag like magnetizing reactance and switching time. As shown in Figs 14 and 15, these two parameters don't affect the voltage sag depth or duration significantly and therefore not considered here.

THE ARTIFICIAL NEURAL NETWORK

There are many types of neural networks for various applications available in the literature [18-25]. Multilayer perceptrons (MLPs) and radial basis functions (RBFs) are examples of feed-forward networks and both universal approximators. In spite of being different networks in several important respects, these two neural network architectures are capable of accurately mimicking each other.

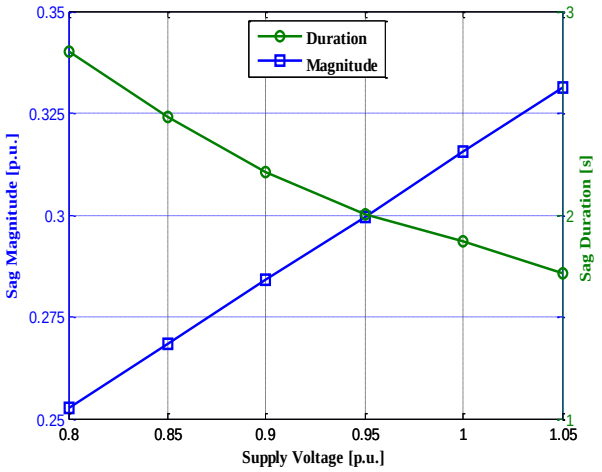

Fig. 5 - Voltage sag magnitude and duration as supply voltage while cable resistance 0.016 p.u., cable reactance 0.0314 p.u., stator resistance 0.008 p.u., stator reactance 0.04 p.u., referred rotor resistance 0.006 p.u., referred rotor reactance 0.04 p.u., load torque 15 N.m, and total inertia 2.9 kg.m^2.

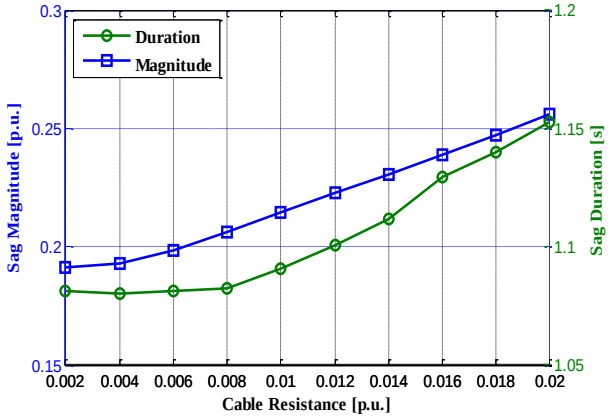

Fig. 6 - Voltage sag magnitude and duration as cable resistance while supply voltage 1 p.u., cable reactance 0.0188 p.u., stator resistance 0.012 p.u., stator reactance 0.04 p.u., referred rotor resistance 0.008 p.u., referred rotor reactance 0.04 p.u., load torque 10 N.m, and total inertia 2.9 kg.m^2.

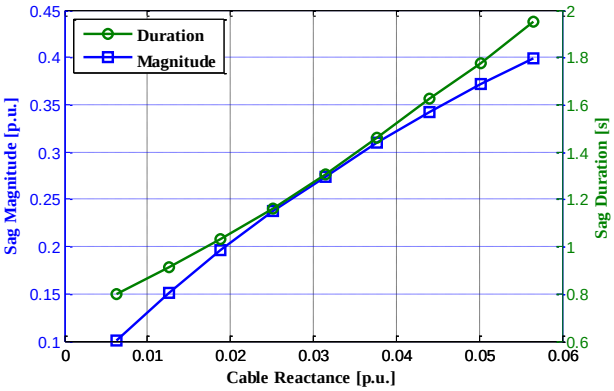

Fig. 7 - Voltage sag magnitude and duration as cable reactance while supply voltage 0.95 p.u., cable resistance 0.008 p.u., stator resistance 0.01 p.u., stator reactance 0.06 p.u., referred rotor resistance 0.008 p.u., referred rotor reactance 0.02 p.u., load torque 10 N.m, and total inertia 2.5 kg.m^2.

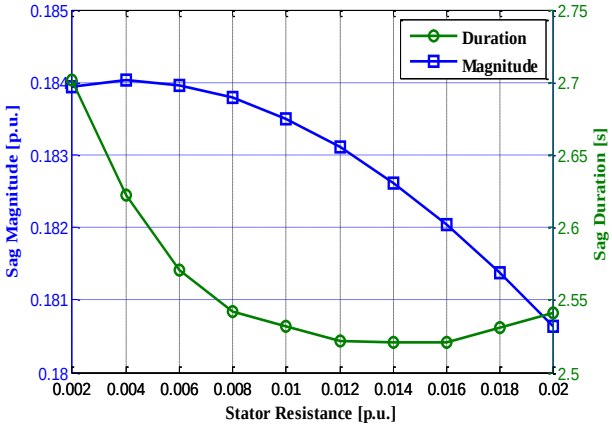

Fig. 8 - Voltage sag magnitude and duration as stator resistance while supply voltage 0.95 p.u., cable resistance 0.008 p.u., cable reactance 0.0314 p.u., stator reactance 0.08 p.u., referred rotor resistance 0.01 p.u., referred rotor reactance 0.06 p.u., load torque 25 N.m, and total inertia 2.5 kg.m^2.

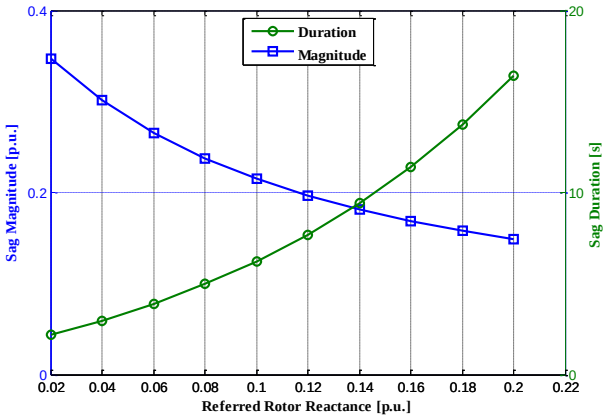

Fig. 11 - Voltage sag magnitude and duration as referred rotor reactance while supply voltage 1.05 p.u., cable resistance 0.01 p.u., cable reactance 0.0377 p.u., stator resistance 0.01 p.u., stator reactance 0.06 p.u., referred rotor resistance 0.006 p.u., load torque 15 N.m, and total inertia 3.5 kg.m^2.

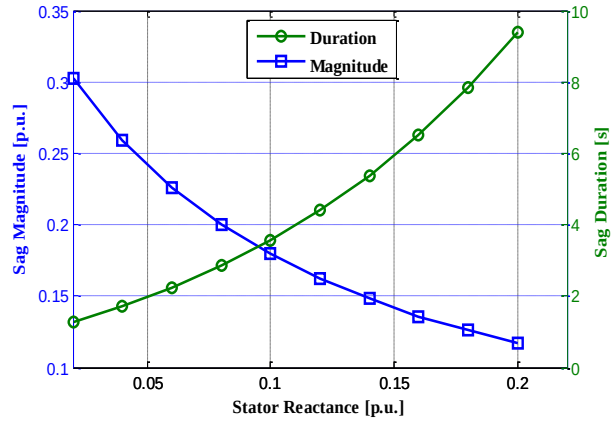

Fig. 9 - Voltage sag magnitude and duration as stator reactance while supply voltage 1 p.u., cable resistance 0.012 p.u., cable reactance 0.0314 p.u., stator resistance 0.01 p.u., referred rotor resistance 0.01 p.u., referred rotor reactance 0.06 p.u., load torque 25 N.m, and total inertia 3.2 kg.m^2.

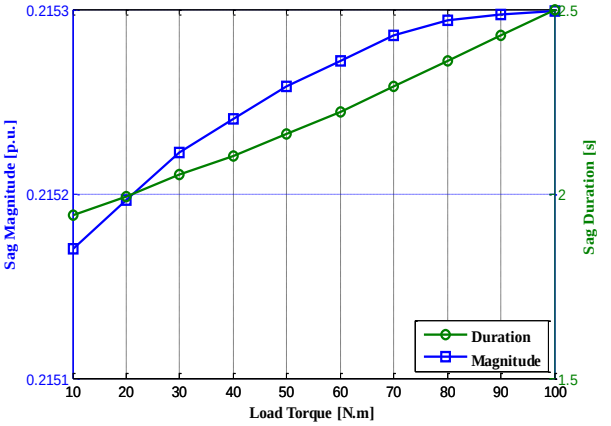

Fig. 12 - Voltage sag magnitude and duration as load torque while supply voltage 1 p.u., cable resistance 0.008 p.u., cable reactance 0.0314 p.u., stator resistance 0.012 p.u., stator reactance 0.08 p.u., referred rotor resistance 0.012 p.u., referred rotor reactance 0.04 p.u., and total inertia 3.5 kg.m^2.

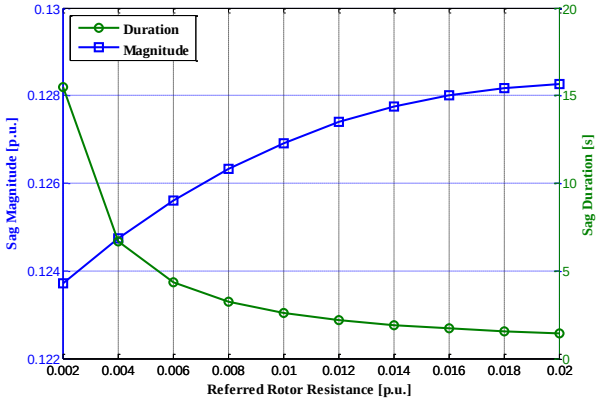

Fig. 10 - Voltage sag magnitude and duration as referred rotor resistance while supply voltage 0.95 p.u., cable resistance 0.01 p.u., cable reactance 0.0188 p.u., stator resistance 0.004 p.u., stator reactance 0.1 p.u., referred rotor reactance 0.04 p.u., load torque 15 N.m, and total inertia 3.2 kg.m^2.

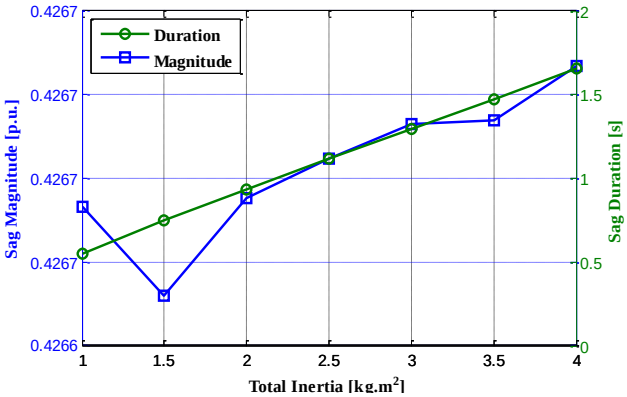

Fig. 13 - Voltage sag magnitude and duration as total inertia while supply voltage 1 p.u., cable resistance 0.008 p.u., cable reactance 0.044 p.u., stator resistance 0.008 p.u., stator reactance 0.04 p.u., referred rotor resistance 0.008 p.u., referred rotor reactance 0.02 p.u., and load torque 20 N.m.

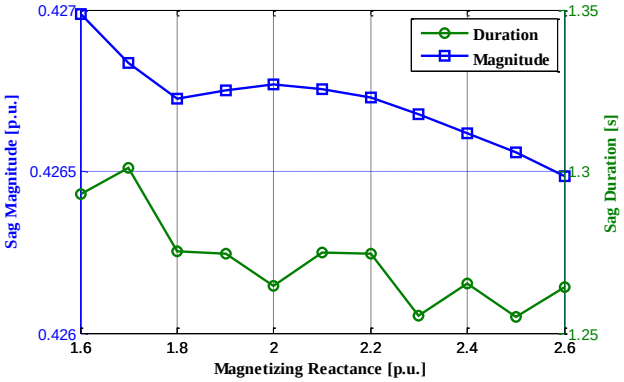

Fig. 14 - Voltage sag magnitude and duration as magnetizing reactance while supply voltage 1 p.u., cable resistance 0.008 p.u., cable reactance 0.044 p.u., stator resistance 0.008 p.u., stator reactance 0.04 p.u., referred rotor resistance 0.008 p.u., referred rotor reactance 0.02 p.u., load torque 20 N.m, and total inertia 2.9 kg.m^2.

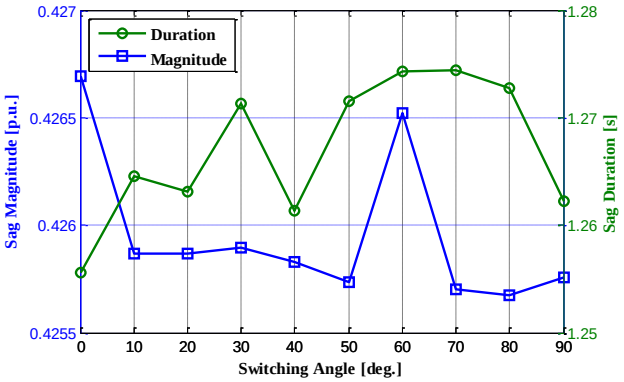

Fig. 15 - Voltage sag magnitude and duration as switching time (angle) while supply voltage 1 p.u., cable resistance 0.008 p.u., cable reactance 0.044 p.u., stator resistance 0.008 p.u., stator reactance 0.04 p.u., referred rotor resistance 0.008 p.u., referred rotor reactance 0.02 p.u., load torque 20 N.m, and total inertia 2.9 kg.m^2.

In this work, different algorithms were used to train MLP structure: back propagation (BP), delta-bar-delta (DBD), extended delta-bar-delta (EDBD), directed random search (DRS), quick propagation (QP), and levenberg–marquardt (LM). Because of space limitation, these structures and related algorithms are not described here. The mathematical background of BP, DBD, EDBD, DRS, QP, and RBF can be found in [18], and LM algorithm is fully discussed in [26]. The basic structure of developed artificial neural network is shown in Fig. 16.

A. Training of ANN

Parameters listed in Section 3 are adopted as ANN inputs and worst case of voltage sag magnitude and duration among three phases are selected as ANN outputs. To train ANNs, all experiments have been repeated for different system parameters. For producing learning and testing sets, ANN inputs were varied in different steps (depend on the parameter). 20% of these sets were used for ANN learning and 80% of these sets were used for ANN testing. Each ANN is trained with the goal of mean square error (MSE) 1e-6. Fig. 17 shows the training of neural network for all structures. Specifications of ANNs are presented in Table 1. After learning, all parameters of the trained networks have been frozen and then used in the retrieval mode for testing the capabilities of the system on the data not used in learning. The testing data samples have been generated through the PSB program by placing the parameter values not used in learning, by applying different parameters. A large number of testing data have been used to check the proposed method in the most objective way at practically all possible parameters variation. Relative error is calculated by the difference of PSB output and ANN output:

$$\mathrm{Er}_{\mathrm{Relative}}(\%) = \frac{|\mathrm{O}_{\mathrm{ANN}} - \mathrm{O}_{\mathrm{PSB}}|}{\mathrm{O}_{\mathrm{PSB}}} \times 100 \qquad (1)$$

and absolute error is calculated as:

$$\mathrm{Er}_{\mathrm{Absolute}} = |\mathrm{O}_{\mathrm{ANN}} - \mathrm{O}_{\mathrm{PSB}}|, \qquad (2)$$

where $\mathrm{O}_{\mathrm{ANN}}$ is the voltage sag depth and duration calculated by ANN, and $\mathrm{O}_{\mathrm{PSB}}$ refers to voltage sag depth and duration calculated by PSB.

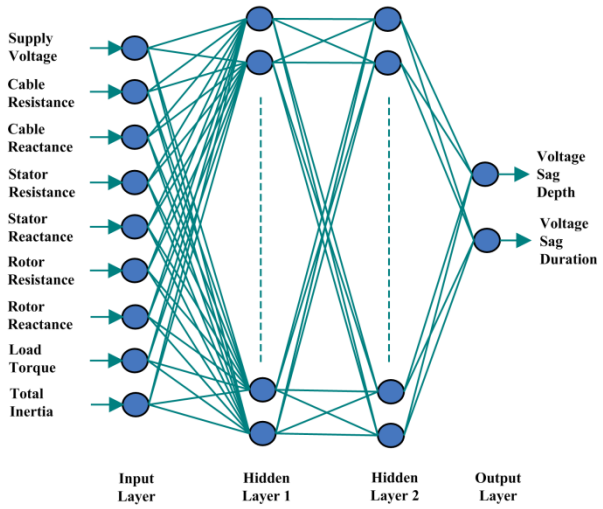

Fig. 16 - Basic structure of developed artificial neural network.

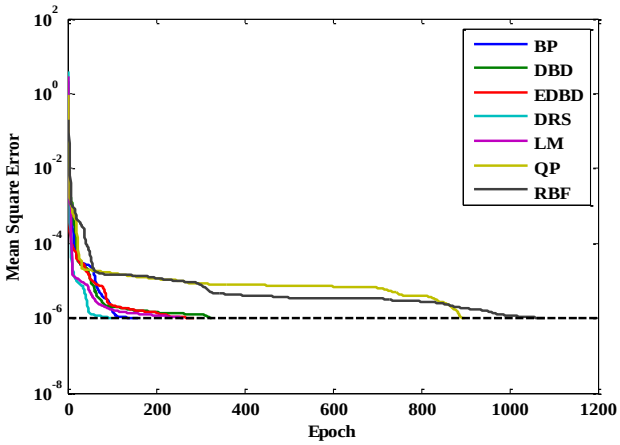

Fig. 17 - Squared error against epoch curve for developed ANNs.

TABLE 1
SPECIFICATIONS OF DEVELOPED ANNS

ANN model	Number of hidden layers	Number of neurons in the hidden layer	Training time [epochs]
BP	2	12	158
DBD	3	14	326
EDBD	3	19	287
DRS	3	12	99
LM	2	17	261
QP	3	14	898
RBF	2	15	1081

Fig. 18 shows relative errors for training and testing sets for LM algorithm. Moreover, results for a sample test data for all developed ANNs are presented in Tables 2 and 3, and Figs. 19-20. Tables 2 presents voltage sag depth calculated using PSB and developed ANNs for some sample data, while Table 3 shows voltage sag duration for same data. Calculated errors for different ANNs in Tables 2 and 3 are relative errors. In the other hand, Fig. 19 shows voltage sag magnitude and duration against the cable resistance, and Fig. 20 presents voltage sag against the rotor reactance.

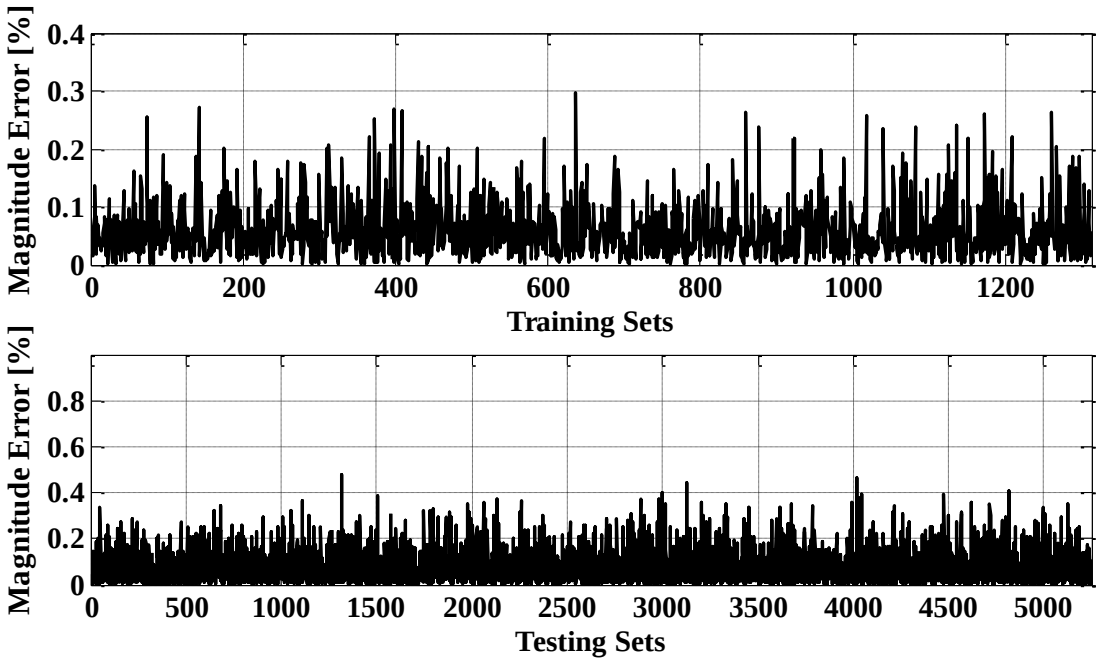

(a)

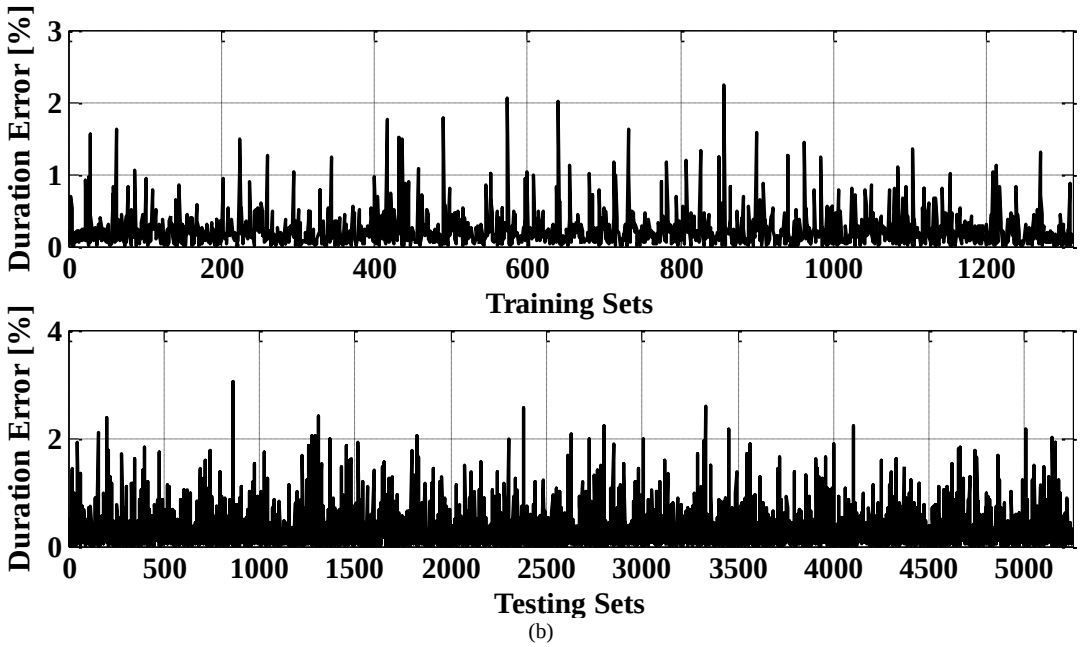

(b)

Fig. 18 - Relative errors of learning and testing sets for LM algorithm. (a) sag depth, (b) sag duration.

TABLE 2
VOLTAGE SAG DEPTH FOR SOME SAMPLE TESTING DATA CALCULATED BY PSB AND DEVELOPED ANNS

V [p.u.]	0.95	0.95	0.95	0.95	1	1	1	1	1.05	1.05	1.05	1.05
R_c [p.u.]	0.006	0.01	0.01	0.01	0.01	0.018	0.018	0.022	0.022	0.022	0.016	0.016
X_c [p.u.]	0.044	0.044	0.044	0.0189	0.0189	0.0189	0.0189	0.0063	0.0063	0.0063	0.0063	0.025
R_s [p.u.]	0.008	0.008	0.002	0.002	0.002	0.002	0.014	0.014	0.014	0.006	0.006	0.006
X_{ls} [p.u.]	0.02	0.04	0.04	0.04	0.08	0.08	0.08	0.08	0.02	0.02	0.02	0.02
R'_r [p.u.]	0.008	0.008	0.008	0.014	0.014	0.014	0.014	0.004	0.004	0.004	0.004	0.01
X'_{lr} [p.u.]	0.02	0.02	0.02	0.04	0.04	0.06	0.06	0.06	0.06	0.08	0.08	0.08
T_L [N.m]	5	5	15	15	15	15	25	25	25	25	35	35
J [kg.m^2]	2	2	2	2.5	2.5	2.5	3	3	3	3.5	3.5	3.5
PSB [p.u.]	0.490899	0.40681	0.413059	0.204935	0.153741	0.151216	0.155928	0.102038	0.203831	0.15039	0.120078	0.250851
LM [p.u.]	0.490682	0.406652	0.412772	0.204631	0.153652	0.15143	0.155888	0.101896	0.204062	0.150583	0.11997	0.250891
Error [%]	0.044179	0.038972	0.069521	0.148178	0.057761	0.141485	0.02505	0.138751	0.113151	0.12849	0.090358	0.016105
EDBD[p.u.]	0.489977	0.407489	0.413188	0.205275	0.153884	0.151126	0.156091	0.101868	0.204051	0.150468	0.119993	0.250945
Error [%]	0.187975	0.166752	0.031048	0.166086	0.092828	0.059738	0.104661	0.166326	0.107826	0.051966	0.070808	0.037348
BP [p.u.]	0.490404	0.405607	0.412726	0.205235	0.153545	0.151113	0.156401	0.102214	0.203454	0.150774	0.120307	0.251448
Error [%]	0.100913	0.295868	0.080728	0.146201	0.127642	0.067989	0.303652	0.172296	0.185144	0.254894	0.190533	0.238182
DBD [p.u.]	0.490185	0.4081	0.412039	0.205473	0.153127	0.151127	0.15649	0.101872	0.20358	0.150819	0.119946	0.250204
Error [%]	0.145587	0.317066	0.246927	0.262325	0.399507	0.058698	0.360991	0.162247	0.123371	0.284902	0.110476	0.257865
QP [p.u.]	0.486617	0.405816	0.414991	0.204305	0.155311	0.150481	0.154918	0.102302	0.20292	0.150575	0.119672	0.251957
Error [%]	0.872249	0.244387	0.467684	0.307309	1.021093	0.486069	0.647448	0.259424	0.447152	0.122775	0.33806	0.440873
RBF [p.u.]	0.493199	0.412306	0.415903	0.207792	0.152002	0.152158	0.155989	0.101651	0.199842	0.148162	0.119436	0.252629
Error [%]	0.468527	1.350961	0.68838	1.394019	1.1316	0.622876	0.039334	0.379191	1.957225	1.481917	0.535062	0.708853
DRS [p.u.]	0.49753	0.400115	0.40959	0.213638	0.157847	0.149208	0.152184	0.099236	0.211916	0.155454	0.123362	0.255578
Error [%]	1.35065	1.6457	0.839841	4.246631	2.670454	1.327855	2.400847	2.746054	3.966394	3.367194	2.73471	1.884496

TABLE 3
VOLTAGE SAG DURATION FOR SOME SAMPLE TESTING DATA CALCULATED BY PSB AND DEVELOPED ANNS

V [p.u.]	0.95	0.95	0.95	0.95	1	1	1	1	1.05	1.05	1.05	1.05
R_c [p.u.]	0.006	0.01	0.01	0.01	0.01	0.018	0.018	0.022	0.022	0.022	0.016	0.016
X_c [p.u.]	0.044	0.044	0.044	0.0189	0.0189	0.0189	0.0189	0.0063	0.0063	0.0063	0.0063	0.025
R_s [p.u.]	0.008	0.008	0.002	0.002	0.002	0.002	0.014	0.014	0.014	0.006	0.006	0.006
X_{ls} [p.u.]	0.02	0.04	0.04	0.04	0.08	0.08	0.08	0.08	0.02	0.02	0.02	0.02
R'_r [p.u.]	0.008	0.008	0.008	0.014	0.014	0.014	0.014	0.004	0.004	0.004	0.004	0.01
X'_{lr} [p.u.]	0.02	0.02	0.02	0.04	0.04	0.06	0.06	0.06	0.06	0.08	0.08	0.08
T_L [N.m]	5	5	15	15	15	15	25	25	25	25	35	35
J [kg.m^2]	2	2	2	2.5	2.5	2.5	3	3	3	3.5	3.5	3.5
PSB [s]	0.693221	0.991326	1.033664	0.678283	1.121686	1.380216	1.702152	5.22253	1.711853	2.701318	2.72934	1.560378
LM [s]	0.697634	0.988735	1.032823	0.67579	1.124365	1.388423	1.704371	5.230161	1.718209	2.708315	2.73394	1.553447
Error [%]	0.636582	0.261322	0.081403	0.367585	0.238788	0.594582	0.130362	0.146121	0.371302	0.259	0.168539	0.444187
EDBD [s]	0.689189	0.983897	1.036116	0.682012	1.116978	1.374115	1.693432	5.197602	1.71406	2.710349	2.721282	1.56138
Error [%]	0.581677	0.749398	0.237226	0.54976	0.419757	0.442065	0.51232	0.477319	0.12894	0.334327	0.295244	0.064212
BP [s]	0.696854	0.990871	1.032617	0.66832	1.11708	1.371917	1.70564	5.254847	1.723821	2.665801	2.745847	1.563156
Error [%]	0.523997	0.04589	0.101306	1.468935	0.410646	0.601346	0.204917	0.618787	0.69915	1.314829	0.604789	0.178022
DBD [s]	0.692076	1.006098	1.028077	0.67336	1.127922	1.377235	1.692991	5.176611	1.70361	2.704002	2.787391	1.553883
Error [%]	0.165235	1.490186	0.540501	0.725878	0.555907	0.216046	0.538235	0.879258	0.481499	0.099344	2.126925	0.416214
QP [s]	0.712538	1.00152	1.02818	0.694801	1.125787	1.364725	1.712116	5.316908	1.702301	2.7489	2.704272	1.539847
Error [%]	2.786499	1.028369	0.530611	2.435186	0.365608	1.122408	0.585341	1.807135	0.557976	1.761409	0.918483	1.315737
RBF [s]	0.680784	1.00469	1.041443	0.693741	1.08899	1.389468	1.75696	5.298589	1.66312	2.630464	2.76158	1.619842
Error [%]	1.794141	1.348105	0.752565	2.279025	2.914929	0.670261	3.219897	1.456357	2.846789	2.622946	1.181209	3.810887
DRS [s]	0.703744	1.040594	1.016076	0.704919	1.068312	1.485394	1.592077	5.457929	1.57412	2.929754	2.599391	1.500641
Error [%]	1.517937	4.969974	1.701578	3.92694	4.758407	7.62039	6.466808	4.507374	8.045832	8.45645	4.761199	3.828376

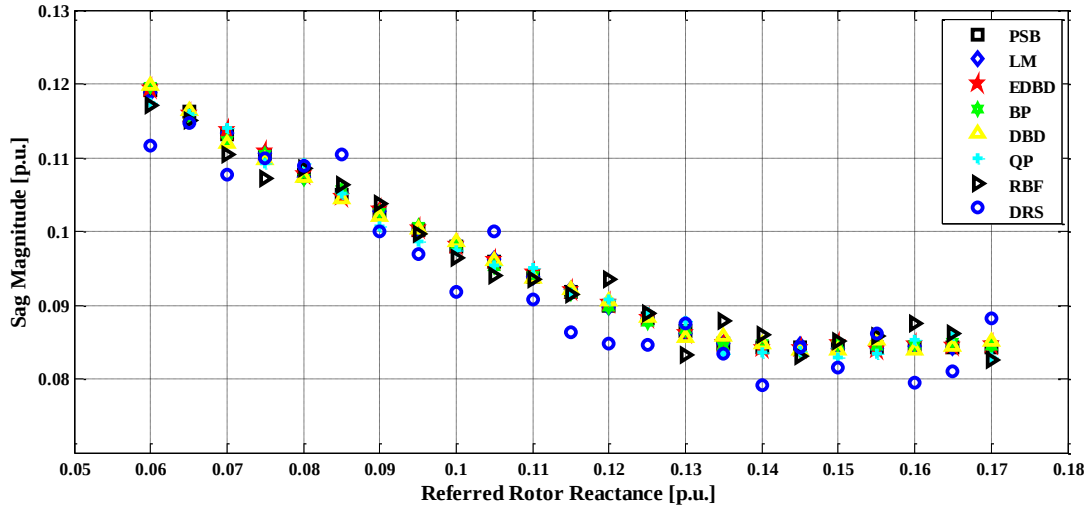

(a)

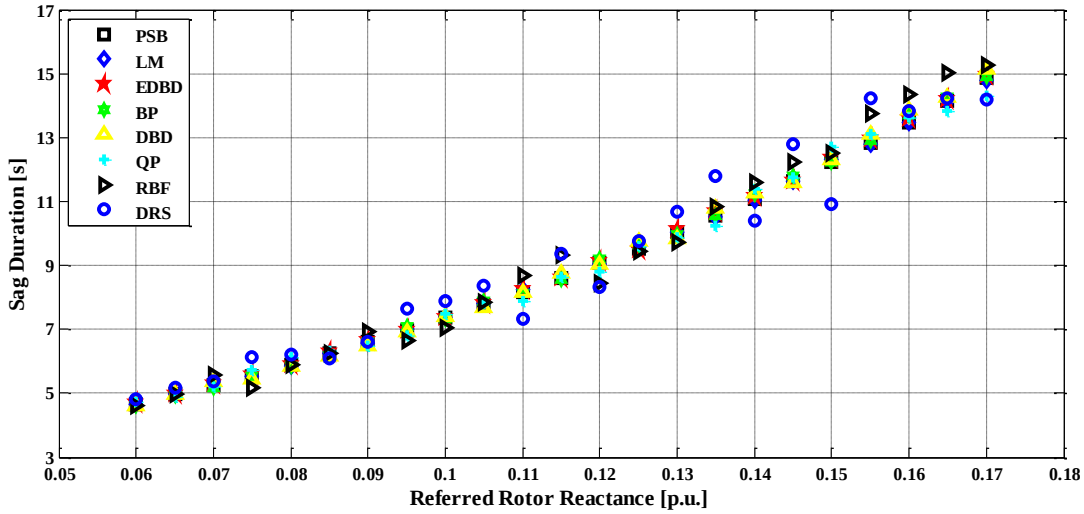

(b)

Fig. 20 - Voltage sag vs. referred rotor reactance simulated by ANNs and PSB while supply voltage 1 p.u., cable resistance 0.01 p.u., cable reactance 0.0188 p.u., stator resistance 0.01 p.u., stator reactance 0.1 p.u., referred rotor resistance 0.006 p.u., load torque 15 N.m, and total inertia 3 kg.m^2. (a) depth, (b) duration.

DISCUSSION

In this paper, voltage sag characteristics evaluated using BP, DBD, EDBD, DRS, QP, LM and RBF neural networks. As can be seen in the Tables 2 and 3, all trained ANNs can estimate voltage sag depth and duration with proper accuracy. To select best approach for voltage sag evaluation, a comparison has been made. Table 4 presents a comparison between these methods based on average of relative and absolute errors for Tables 2 and 3 sample data. It can be seen from Table 4 that LM and EDBD algorithms have better performance (smaller relative and absolute errors) to evaluate both magnitude and duration of voltage sag caused by induction motors starting.

CONCLUSION

This paper presents an artificial neural network-based approach to evaluate voltage sag caused by induction motors starting. Both MLP and RBF structures have been employed for this purpose. MLP is trained with BP, DBD, EDBD, DRS, QP, and LM algorithms. Simulation results show that all developed ANNS can estimate voltage sag characteristics; however LM and EDBD algorithms present better accuracy.

This technique can help the companies and operators to evaluate voltage sag during both design and operation stages real-time to enhance power quality of sensitive loads.

Acknowledgements

This work was supported by the Iran's National Elites Foundation.

REFERENCES

[1] J.V. Milanovic, M.T. Aung, S.C. Vegunta, "The Influence of Induction Motors on Voltage Sag Propagation—Part I: Accounting for the Change in Sag Characteristics," *IEEE Transactions on Power Delivery*, vol. 23, no. 2, pp.1063-1071, Apr. 2008.

[2] C.J. Sr. Melhorn, A. Maitra, W. Sunderman, M. Waclawiak, A. Sundaram, "Distribution system power quality assessment phase II: voltage sag and interruption analysis," in *Proc. Petroleum and Chemical Industry Conference, 2005. Industry Applications Society 52nd Annual*, pp. 113-120, 12-14 Sept. 2005.

[3] J. C. Gomez, C. Reineri, G. Campetelli, M.M. Morcos, "A Study of Voltage Sags Generated by Induction Motor Starting," *Electric Power Components and Systems*, vol. 32, no. 6, 2004.

[4] M. H. Moradi and Y. Mohammadi, "A new current-based method for voltage sag source location using directional overcurrent relay information," *International Transactions on Electrical Energy Systems*, vol. 23, no. 2, pp. 270–281, Mar. 2013.

[5] A. Foroughi, E. Mohammadi, S. Esmaeili, "Application of HH-transform and support vector machine for detection and classification of voltage sag sources," *Turkish Journal of Electrical Engineering & Computer Sciences*, to be published.

[6] Z. Moravej, M. Pazoki, M. Niasati, A.A. Abdoos, "A hybrid intelligence approach for power quality disturbances detection and classification," *International Transactions on Electrical Energy Systems*, vol. 23, no. 7, pp. 914–929, 2013.

[7] S. Kamble and C. Thorat, "Characteristics Analysis of Voltage Sag in Distribution System using RMS Voltage Method," *ACEEE Int. J. on Electrical and Power Engineering*, vol. 3, no. 1, pp. 55-61, Feb 2012.

[8] "IEEE Recommended Practice for Monitoring Electric Power Quality," IEEE Std. 1159-1995, June 1995.

[9] "Testing and measurement techniques – Power quality measurement methods," IEC 61000-4-30, 2003.

[10] M. Ito, H. Okuda, N. Takahashi, and T. Miyata, "Starting current analysis of three-phase squirrel-cage induction motor by finite element method", *Electrical Engineering in Japan*, vol. 99, pp. 36–42, 1979.

[11] *J. Buksnaitis*, "Analytical Determination of Mechanical Characteristics of Asynchronous Motors by Varying the Electric Current Frequency", *Electronics and Electrical Engineering (Elektronika ir Elektrotechnika)*, vol. 112, pp. 3-6, 2011.

[12] A. Ketabi and I. Sadeghkhani, *Electric Power Systems Simulation Using MATLAB*. 2nd Edition, Morsal Publications, Kashan, Iran, Oct. 2012. (in Persian)

[13] P. C. Krause, O. Wasynczuk, S. D. Sudhoff, and S. Pekarek, *Analysis of Electric Machinery and Drive Systems*. 3rd Edition, Wiley-IEEE Press, Jul. 2013.

[14] I. Sadeghkhani, A. Ketabi, and R. Feuillet, "Investigation of Transmission Line Models for Switching Overvoltages Studies", *International Journal of Emerging Electric Power Systems*, vol. 14, pp. 231-238, July. 2013.

[15] L. Wang, C.N.M. Ho, F. Canales, and J. Jatskevich, "High-Frequency Modeling of the Long-Cable-Fed Induction Motor Drive System Using TLM Approach for Predicting Overvoltage Transients", *IEEE Transactions on Power Electronics*, vol. 25, pp. 2653 – 2664, Oct. 2010.

[16] [Online]. Available: www.valiadis.gr/pool/ftp/drawings/KHV355-2_200KW_3300V_TEST_REPORT.pdf.

[17] P.C. Sen, *Principles of Electric Machines and Power Electronics*. 2nd Edition, John Willey, Jan. 1997.

[18] C. Yildiz, S. Gultekin, K. Guney, and S. Sagiroglu, "Neural Models for the Resonant Frequency of Electrically Thin and Thick Circular Microstrip Antennas and the Characteristic Parameters of Asymmetric Coplanar Waveguides Backed with a Conductor", *AEU - International Journal of Electronics and Communications*, vol. 56, pp.396–406, 2002.

[19] I. Sadeghkhani and A. Ketabi, *Switching Overvoltages during Restoration: Evaluation and Control Using ANN*. Lambert Academic Publishing, Köln, Germany, Aug. 2012.

[20] A. Askarzadeh, "Voltage prediction of a photovoltaic module using artificial neural networks," *International Transactions on Electrical Energy Systems*, 2013. doi: 10.1002/etep.1799.

[21] S. Anbazhagan, N. Kumarappan, "Day-Ahead Deregulated Electricity Market Price Forecasting Using Recurrent Neural Network," *IEEE Systems Journal*, vol. 7, no. 4, pp. 866-872, Dec. 2013.

[22] A. Ketabi, I. Sadeghkhani, and R. Feuillet, "Using Artificial Neural Network to Analyze Harmonic Overvoltages during Power System Restoration," *European Transactions on Electrical Power*, vol. 21, no. 7, pp. 1941-1953, Oct. 2011

[23] A.N. Al-Masri, M.Z.A. Ab Kadir, H. Hizam, N. Mariun, "A Novel Implementation for Generator Rotor Angle Stability Prediction Using an Adaptive Artificial Neural Network Application for Dynamic Security Assessment," *IEEE Transactions on Power Systems*, vol. 28, no. 3, pp. 2516-2525, Aug. 2013.

[24] R. Sunitha, S.K. Kumar, A.T. Mathew, "Online Static Security Assessment Module Using Artificial Neural Networks," *IEEE Transactions on Power Systems*, vol. 28, no. 4, pp. 4328 - 4335, Nov. 2013.

[25] Z. He, H. Zhang, J. Zhao, Q. Qian, "Classification of power quality disturbances using quantum neural network and DS evidence fusion*," European Transactions on Electrical Power*, vol. 22, no. 4, pp. 533–547, May 2012.

[26] M. T. Hagan and M. B. Menhaj, "Training feedforward networks with the Marquardt algorithm", *IEEE Trans. Neural Network*, vol.5+, pp. 989-993, Nov. 1994.